Thermodynamics of the DNA Binding Reaction of Transcription Factor MASH-1†

Andreas G. E. Künne,‡,§ Martin Sieber,‡ Daniel Meierhans, and Rudolf K. Allemann*

Department of Chemistry, ETH-Zurich, Universitätstrasse 16, CH-8092 Zurich, Switzerland

Received October 14, 1997; Revised Manuscript Received November 26, 1997

ABSTRACT: MASH-1, a member of the basic helix−loop−helix (BHLH) family of transcription factors, promotes the differentiation of committed neuronal precursor cells. We have determined the thermodynamic parameters of the DNA binding reaction of the BHLH domain of MASH-1 (MASH−BHLH) by isothermal titration calorimetry and found that the specificity of the binding reaction was rather low. At 27 °C, the association constant for binding was 5.13 (±0.51) × 10^8 M^{-1} for an E-box containing oligonucleotide, while for a heterologous DNA sequence it was 5.14 (±1.93) × 10^7 M^{-1}. The reaction enthalpy and the reaction entropy were strongly dependent on the temperature, but the reaction free energy was almost independent of temperature. The association reaction was enthalpically driven throughout the physiological temperature range and characterized by a large negative heat capacity change. No change in the protonation state of the protein and/or the DNA was observed at pH 6. Within experimental error, the reaction was independent of pH between pH 6 and 8. Dissection of the entropy change of the binding reaction indicated that binding was coupled to local protein folding of approximately 25 amino acids per protein subunit. The circular dichroism spectra of free and DNA-bound MASH−BHLH revealed the formation of additional α-helical structure comprising approximately 25 amino acids upon complex formation. Therefore, while the basic region was in an α-helical conformation in the DNA complex, in free MASH−BHLH it was substantially unfolded even at concentrations where the protein is mainly dimeric. The association between MASH-1 and DNA is therefore an example of "induced fit".

Many of the members of the basic helix−loop−helix (BHLH)[1] family of transcription factors (Figure 1A) are involved in the control of cellular differentiation. For example, the expression of the BHLH protein MASH-1 commits cells to a neural fate (*1*), while MyoD, myogenin, MRF4, and Myf-5 can activate the program for skeletal muscle differentiation in a wide range of different cell types (*2*). The SCL protein, on the other hand, appears to have a fundamental role in erythroid differentiation (*3*). For functional activity, the myogenic and the neurogenic BHLH proteins depend on the ubiquitously expressed E2A gene products E12 and E47, which are themselves BHLH proteins (*4*, *5*).

The BHLH proteins are named after a common region of high sequence similarity called the BHLH domain (Figure 1A) through which they dimerize and bind to DNA. The HLH region which mediates dimerization consists of two α-helixes connected by a flexible loop. This region forms a parallel, left-handed, four-helix bundle in the DNA complex (*6*, *7*). The activity of BHLH proteins as transcriptional activators depends on the presence of DNA sequences containing the symmetrical core motif CANNTG (Figure 1B), which is called an E-box (*8*). The X-ray structures of the complexes of E47 and MyoD revealed that one DNA half-site is contacted through amino acid residues of the basic region of one BHLH subunit while the other half-site interacts with the basic region of the other subunit. In structural terms, the basic region is simply the amino-terminal end of one α-helix consisting of the basic region and helix 1. X-ray structure analyses of the DNA complexes of BHLH proteins suggest that in most cases the DNA remains in the canonical B conformation (*6*, *7*, *9*−*11*).

Surprisingly, DNA binding studies by EMSA and by CD spectroscopy showed that the BHLH proteins MASH-1, MyoD, and E12 display only modest DNA binding specificity and that their binding preferences for different E-box sequences are similar (*12*, *13*). In the absence of DNA, the BHLH domain of MASH-1 (MASH−BHLH) (Figure 1A) is largely disordered at the concentrations where DNA binding occurs (*12*, *14*). However, upon binding to DNA, MASH−BHLH adopts a mainly α-helical conformation. It appears therefore that folding of the BHLH domain of MASH-1 and DNA binding are coupled processes.

Despite the important role played by the BHLH proteins in transcriptional activation and cellular differentiation and the many studies of their DNA binding, no comprehensive characterization exists of the thermodynamics of their

† This work was supported by an ETH grant (to R.K.A. and A.G.E.K.).

* Author to whom correspondence should be addressed. Phone +41-1-632 2895. Fax: +41-1-632 2911. E-mail: ALLEMANN@chem.ethz.ch.

‡ These authors have contributed equally to this work.

§ Present address: Molecular Parasitology, Institute of Molecular Medicine, John Radcliffe Hospital, Oxford OX3 9DU, United Kingdom.

[1] Abbreviations: BHLH, basic helix−loop−helix; CD, circular dichroism; EMSA, electrophoretic mobility shift assay; HPLC, high-performance liquid chromatography; IgH, immunoglobulin H; ITC, isothermal titration calorimetry; MALDI-TOF, matrix-assisted laser desorption time-of-flight; MASH, mammalian achaete-scute homologue; MASH−BHLH, BHLH domain of MASH-1 comprising amino acids 106−172 of MASH-1 plus an exogenous proline at the carboxy terminus; MCK, muscle creatine kinase; MEF, myocyte enhancer factor.

S0006-2960(97)02537-3 CCC: $15.00
Published on Web 02/28/1998

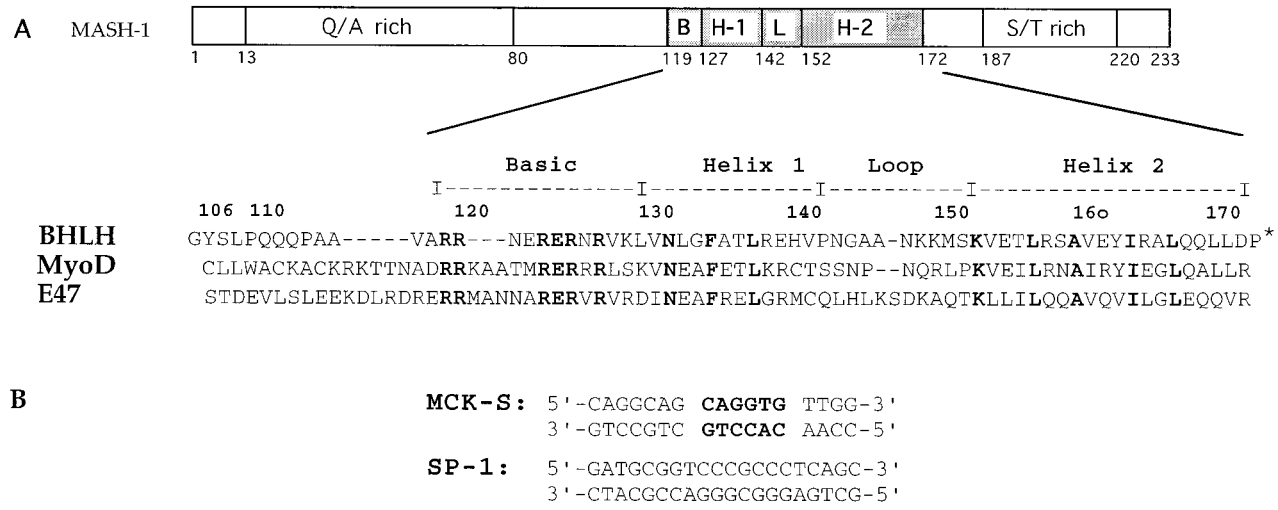

FIGURE 1: (A) Cartoon of the MASH-1 protein and sequence similarities between the BHLH domains of MASH-1 (MASH−BHLH), MyoD, and E47. The numbering system indicated for the MASH−BHLH sequence corresponds to the full-length MASH-1 sequence. The proline residue at the carboxy end of MASH−BHLH is a cloning artifact and is not part of the MASH-1 sequence. The positions of the basic region, helix 1, helix 2, and the interconnecting loop are based on the crystal structure of the DNA complex of the BHLH domain of MyoD (*6*). The sequences of MASH-1 (*5*) and of E47 (*49*) are from rat; for MyoD, the murine sequence is given (*50*). (B) Sequences of the double-stranded oligonucleotides MCK-S and SP-1. The E-box sequence is shown in bold-face.

association with DNA. Thermodynamic studies provide a description of the forces which drive the reaction between proteins and DNA (*15*). Together with structural studies, they enable us to understand the association reaction in physical terms.

We have used isothermal titration calorimetry (ITC) to study the binding of MASH−BHLH to an E-box-containing oligonucleotide, MCK-S, comprising 17 bp of IgH enhancer like element of the muscle-specific creatine kinase enhancer (*16*) and to heterologous DNA. These measurements confirmed the low DNA binding specificity of MASH−BHLH under true equilibrium conditions. Dissection of the entropy changes of the binding reaction indicated that local protein folding transitions were coupled to DNA binding. We propose that the basic region of MASH−BHLH is substantially unfolded even at the high concentrations used here, but adopts an α-helical conformation on binding to DNA. This folding transition is driven by binding free energy, and therefore is an example of "induced fit" and adaptability.

EXPERIMENTAL PROCEDURES

Expression and Purification of MASH-1 BHLH. The BHLH domain of rat MASH-1 comprising amino acids 106 through 172 was produced in BL21(DE3)pLysS cells from the T7 promoter in the plasmid pJGetita and purified as described (*12*). The protein contains an additional proline residue at the carboxy-terminal end which is due to the cloning procedure and is not part of the MASH-1 sequence (*12*). SDS−gel electrophoresis of the purified product showed a single band. MALDI-TOF mass spectroscopy revealed a molecular mass of 7700 u which corresponded well with the calculated mass of 7698.8 u for MASH−BHLH lacking the N-terminal methionine. Edman sequencing confirmed the lack of the N-terminal methionine as well as the identity of the first eight amino acid residues of the recombinant protein. The protein concentration was determined by measuring the UV absorption at 215 and 220 nm (*17*).

Oligonucleotides. Oligonucleotides were purchased from Microsynth or the University of Zurich (Institute for Zoology), desalted on Sephadex, and precipitated with ethanol. For electrophoretic mobility shift assays, single-stranded oligonucleotides were labeled with [γ-^{32}P]ATP (Amersham) in the presence of T4 polynucleotide kinase (New England Biolabs). Complementary strands were annealed by heat denaturation followed by slow cooling to room temperature.

Electrophoretic Mobility Shift Assays. Electrophoretic mobility shift assays were performed as previously described (*12*−*14*). Bacterially expressed MASH−BHLH was serially diluted into EMSA buffer (50 mM Tris-HCl, pH 8; 50 mM MOPS, pH 7; or 50 mM MES, pH 6, respectively, 6 mM $MgCl_2$, 40 mM ammonium sulfate, 0.2 mM EDTA, 1 mM DTT, 5% glycerol). This solution was incubated in the presence of 10 nM labeled oligonucleotide for 10 min at RT. Samples were applied to 4% polyacrylamide gels in 0.9 × TAE (pH 7.9). After electrophoresis, the gels were dried and exposed to Kodak X-OMAT-S film at −70 °C. Quantitative data were obtained with a Packard Instantimager using system software. The fraction, Φ, of DNA bound was determined as the activity of the retarded band (corresponding to the protein DNA complex) divided by the sum of the activities of the retarded and unretarded (corresponding to the free DNA) bands. Plotting Φ against the concentration of unbound MASH−BHLH allowed the determination of the concentration $[MASH-BHLH]_{1/2}$, where half of the protein binding sites are filled (*12*−*14*).

Buffers. Low-salt MES buffer: 10 mM MES−KOH, pH 6.0. High-salt MES buffer: 10 mM MES−KOH, pH 6.0, 100 mM KCl. PIPES-6 buffer: 10 mM PIPES−KOH, pH 6.0. PIPES-7 buffer: 10 mM PIPES−KOH, pH 7.0.

Isothermal Titration Calorimetry. ITC measurements were performed on an OMEGA titration calorimeter (MicroCal, Inc., Northampton, MA) at the Institute of Biochemistry of the University of Zurich. The OMEGA calorimeter has been described in detail by Wiseman and co-workers (*18*). The calorimeter was calibrated with electrically generated heat pulses as recommended by the manufacturer.

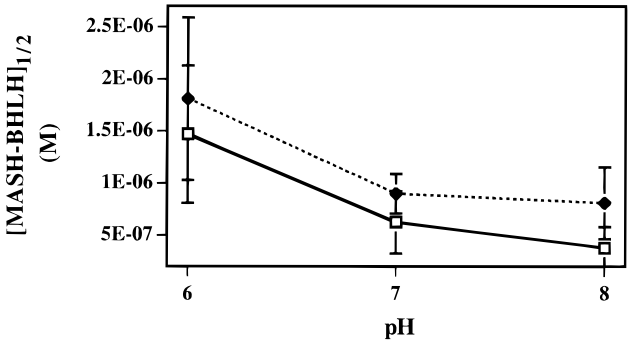

FIGURE 2: pH dependence of the interaction between MASH−BHLH and the MCK-S (□) and SP-1 (◆) oligonucleotides measured by EMSA. The concentration of MASH−BHLH, $[MASH-BHLH]_{1/2}$, at which half of the DNA binding sites are filled is given for the pH range from 6 to 8.

The temperature of the system was kept 5 °C below the temperature of the experiment with the help of a circulating water bath in order to improve base line stability. Temperature equilibration was allowed to proceed for approximately 12 h. All solutions used in ITC experiments were degassed by evacuation. Samples of MASH−BHLH and DNA were extensively dialyzed against the same batch of buffer to minimize artifacts as a consequence of minor differences in buffer composition. The reaction cell contained 1.33 mL of 5 μM DNA in reaction buffer. The injection syringe contained 184 μM MASH−BHLH in buffer and was rotated at 350 rpm during equilibration and experiment. Injections were started after equilibration to base line stability was reached. Titrations consisted of 15 injections of 8 μL and 14.8 s duration. The length of the intervals between injections was 300 s. The titration data were corrected for the small heat changes observed in control titrations of protein into buffer. Data analysis was performed with the software provided with the instrument (*18*). The total heat of binding, ΔH, and the association constant, K_A, for the binding reaction were obtained by nonlinear least-squares fitting of the data to a 1:1 binding model (one BHLH dimer per DNA duplex) utilizing the Marquardt algorithm. Stoichiometries of the fits to the 1:1 binding model agreed to within ±15%.

CD Spectroscopy. Spectra were measured on a Jasco J600 circular dichroism spectrometer at 293 K. For every measurement, MASH−BHLH was freshly diluted from a stock solution into 5 mM PIPES−KOH, pH 7.0. Spectra were measured for a BHLH concentration of 100 μM in a cuvette of 0.1 mm path length. The concentration of the double-stranded oligonucleotide was 50 μM. CD spectra of DNA complexes of MASH−BHLH are reported as difference spectra.

UV Spectroscopy. The optical melting curves were obtained on 5 μM solutions of double-stranded MCK-S and SP-1 oligonucleotide using a Cary 1 Bio spectrophotometer. The annealed DNA was dialyzed several times against high-salt MES buffer as described for the ITC experiments. This solution was transferred to a 1 cm path length quartz cuvette, and mineral oil was layered on top. Absorbance readings at 260 nm were obtained in 1.5 °C increments for the temperature range from 0 °C to 90 °C. A full cycle (0 °C→90 °C→0 °C) lasted 3.5 h, and the reported data are the average of three cycles.

Table 1: Thermodynamic Parameters of the Binding Reaction of MASH−BHLH and Different DNA Binding Sites[a]

T (K)	$K_A \times 10^{-7}$ (M^{-1})	ΔG (kcal/mol)[b]	ΔH (kcal/mol)	$T\Delta S$ (kcal/mol)[c]
		MCK-S in Low-Salt MES Buffer (pH 6.0)		
285	3.41 ± 0.1	−9.8 ± 0.1	−19.8 ± 0.1	−10.0 ± 0.2
290	4.25 ± 0.1	−10.1 ± 0.2	−19.9 ± 1.2	−9.8 ± 1.4
295	17.75 ± 5.8	−11.1 ± 0.2	−26.3 ± 1.8	−15.2 ± 2.0
300	51.25 ± 5.12	−11.9 ± 0.4	−29.8 ± 1.1	−17.9 ± 1.5
305	41.42 ± 6.20	−12.0 ± 0.5	−33.2 ± 1.2	−21.1 ± 1.7
		SP-1 in Low-Salt MES Buffer (pH 6.0)		
285	2.08 ± 0.31	−9.5 ± 0.1	−15.3 ± 0.1	−5.8 ± 0.2
287	2.06 ± 0.22	−9.6 ± 0.1	−17.5 ± 0.1	−7.9 ± 0.2
290	2.31 ± 0.47	−9.8 ± 0.1	−15.5 ± 1.9	−5.7 ± 2.0
295	5.14 ± 6.28	−10.4 ± 0.5	−18.1 ± 2.5	−7.7 ± 3.0
300	5.14 ± 1.93	−10.4 ± 0.3	−25.0 ± 3.1	−14.7 ± 3.4
		MCK-S in High-Salt MES Buffer (pH 6.0)		
290	3.92 ± 0.25	−10.1 ± 0.1	−22.0 ± 0.4	−11.9 ± 0.5
295	2.85 ± 0.77	−10.1 ± 0.2	−24.2 ± 1.6	−14.2 ± 1.8
300	2.24 ± 0.78	−10.1 ± 0.2	−29.4 ± 1.7	−19.3 ± 1.9
		SP-1 in High-Salt MES Buffer (pH 6.0)		
290	2.89 ± 1.86	−9.9 ± 0.4	−18.4 ± 0.7	−8.5 ± 1.1
295	2.55 ± 1.54	−10.0 ± 0.5	−21.4 ± 2.9	−11.4 ± 3.3
300	1.30 ± 0.02	−9.8 ± 0.1	−22.2 ± 0.3	−12.4 ± 0.3

[a] Standard deviations from multiple measurements are given. [b] From K_A: $\Delta G = -RT \ln K_A$. [c] Calculated from $T\Delta S = \Delta H - \Delta G$.

Table 2: Dependence of the Thermodynamic Parameters of the DNA Binding Reaction of MASH−BHLH on Buffer and pH[a]

buffer	pH	T (K)	ΔG[b] (kcal/mol)	ΔH (kcal/mol)	$T\Delta S$[c] (kcal/mol)
			MCK-S		
MES	6.0	295	−11.1 ± 0.2	−26.3 ± 1.8	−15.2 ± 2.0
PIPES	6.0	295	−10.7 ± 0.3	−24.1 ± 0.5	−13.4 ± 0.7
PIPES	7.0	295	−10.6 ± 0.3	−19.6 ± 0.9	−9.0 ± 1.0
			SP-1		
MES	6.0	295	−10.4 ± 0.5	−18.1 ± 2.5	−7.7 ± 3.0
PIPES	6.0	295	−9.8 ± 0.1	−19.8 ± 0.1	−10.0 ± 0.1
PIPES	7.0	295	−10.4 ± 0.3	−14.5 ± 1.4	−4.0 ± 1.7

[a] Standard deviations from multiple measurements are given. [b] From the measurement of K_A: $\Delta G = -RT \ln K_A$. [c] Calculated from $T\Delta S = \Delta H - \Delta G$.

RESULTS AND DISCUSSION

pH Dependence of the Binding Reaction Studied by EMSA. To monitor the effect of pH on the stability of the DNA complexes of MASH−BHLH with oligonucleotides containing an E-box and with heterologous DNA (Figure 1B), the dissociation constants of the complexes were measured in electrophoretic mobility shift assays over the pH range from 6.0 to 8.0. These experiments showed that the position of the equilibrium of the binding reaction was only slightly dependent on the pH of the solution under these experimental conditions (Figure 2). The dissociation constants for the complexes of MASH−BHLH with both MCK-S and SP-1 DNA were slightly smaller at higher pH, while the specificity of the binding reaction was not dependent on the pH of the solution. Given the limited accuracy of thermodynamic data determined by EMSA, these results agreed with the data obtained from isothermal titration calorimetry experiments, which showed that protonation did not take place on complex formation (Table 2) (vide infra). The majority of the ITC experiments described below were therefore performed at

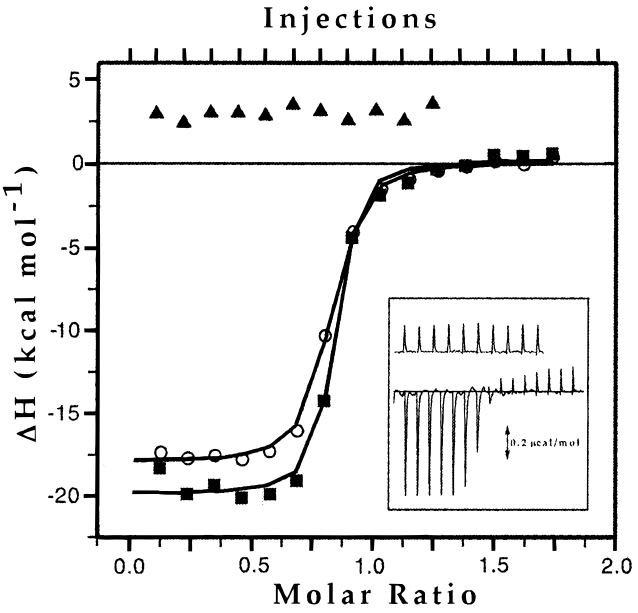

FIGURE 3: Examples of isothermal titrations of MCK-S (■) and SP-1 (○) with MASH−BHLH. 5 μM DNA was titrated with 184 μM MASH−BHLH in low-salt MES buffer at 290 K. Abscissa: moles of MASH−BHLH dimer added per mole of DNA target. Control titration of MASH−BHLH into MES-buffer (▲). Inset: raw data for the titration of MCK-S DNA (lower trace); control titration of MASH−BHLH into low-salt MES buffer (upper trace).

pH 6, a value at which the solubility of MASH−BHLH is sufficiently high even under high-salt conditions.

ITC Measurements of the Binding Reaction. In isothermal titration calorimetry experiments (*18*), the thermodynamic parameters and the stoichiometry of the binding reaction between MASH−BHLH and the MCK-S and SP-1 oligonucleotides were determined by direct measurement of the evolved heat as a function of temperature in the range from 12 °C to 32 °C (Table 1 and Figure 3). For all titrations, the best fit of the experimental data to the binding isotherm was obtained under the assumption of one dimeric MASH−BHLH binding per double-stranded oligonucleotide (Figure 3). Control titration of MASH−BHLH into buffer which did not contain DNA gave rise to small endothermic peaks of equal size within the limits of error (Figure 3). Overtitration with a large excess of MASH−BHLH did not reveal any sign of a second binding site as has been described for other DNA−protein interactions (*19, 20*).

In low-salt MES buffer, the association constants for the binding reaction between MASH−BHLH and MCK-S and SP-1 were $(3.41 \pm 0.1) \times 10^7$ M^{-1} and $(2.08 \pm 0.31) \times 10^7$ M^{-1} at 12 °C and $(51.25 \pm 5.12) \times 10^7$ M^{-1} and $(5.14 \pm 1.93) \times 10^7$ M^{-1} at 27 °C, respectively (Table 1). At 27 °C, the concentration of MASH−BHLH needed to bind half of the MCK-S oligonucleotides is therefore approximately 1 order of magnitude lower than the concentration required for half-maximal binding of the SP-1 oligonucleotide.

The specificity of the binding reaction of MASH−BHLH was similar in low-salt PIPES buffer (Table 2) and with other heterologous DNA sequences (data not shown). The specificity of DNA binding was slightly lower in high-salt buffer at pH 6 and in low-salt buffer at pH 7 (Tables 1 and 2). The measurement of the thermodynamic parameters in high-salt buffer at pH 7 was precluded by the low solubility of MASH−BHLH under these conditions.

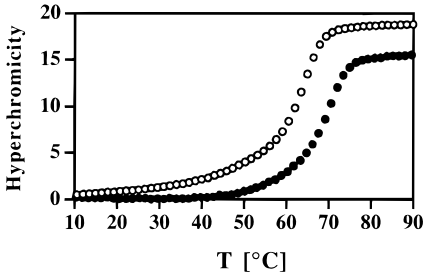

FIGURE 4: Thermal stability of the MCK-S (○) and the SP-1 (●) oligonucleotides. The optical melting profile of a 5 μM solution of the double-stranded oligonucleotides was measured at 260 nm. The hyperchromicity is given as a function of the temperature. Hyperchromicity was calculated as $100 \times [(A_{260}(T) - A_{260}(0\ °C))/A_{260}(0\ °C)]$.

The melting curves of the MCK-S and the SP-1 oligonucleotides at a concentration of 5 μM (the concentration used in the ITC experiments) were measured by UV spectroscopy and showed a sharp transition at approximately 61 and 68 °C, respectively (Figure 4). The hyperchroism was less than 1% at temperatures below 35 °C (Figure 4), indicating that the stability of the duplex DNA did not interfere with the accuracy of the ITC experiments.

The results described above were in good agreement with earlier EMSA experiments which had also revealed that MASH-1 binds to DNA with low sequence specificity (*12*, *14*). They confirmed in a thermodynamically vigorous assay the earlier finding that MASH-1 and most likely many other BHLH proteins display only modest sequence specificity.

It is interesting to discuss the low DNA binding specificity in the context of the crystal structures of the DNA complexes of E47 (*7*) and MyoD (*6*). The high affinity of these BHLH proteins for DNA is a consequence of a large number of contacts formed between the phosphate backbone and amino acid residues. No specific contacts exist between the proteins and the central two base pairs of the E-box. Both in E47 and in MyoD, the carboxylate of a glutamate side chain is hydrogen-bonded to the N(4) of cytosine and the N(6) of adenine. In both subunits of MyoD, additional hydrogen bonds exist between O(6) and N(7) of guanine and one of the N_η of an arginine residue, while in E47 a hydrogen bond is formed between O(6) of guanine and the carbonyl of an asparagine side chain in only one subunit. Obviously, MyoD and E47 rely on only a small number of hydrogen bonds between amino acid residues and the nucleobases for specific DNA recognition, and this might explain the small amount of sequence preference observed with these proteins at least within the context of the moderate resolution of the X-ray structures (*6*, *7*).

Thermodynamic Parameters of the Binding Reaction. The binding reactions between MASH−BHLH and the MCK-S and SP-1 oligonucleotides were strongly exothermic (Tables 1 and 2). In all buffer systems studied, the enthalpies were more negative for binding to E-box-containing DNA than for the reaction with heterologous DNA sequences. The values measured for ΔH in low-salt MES and PIPES buffer were indistinguishable within the accuracy of the measurement, indicating that no important protonation or deprotonation step was involved in the binding reaction (Table 2). Such a change in the protonation state would have led to significantly altered values for ΔH in the two buffers. Similar results were obtained for the DNA binding reactions

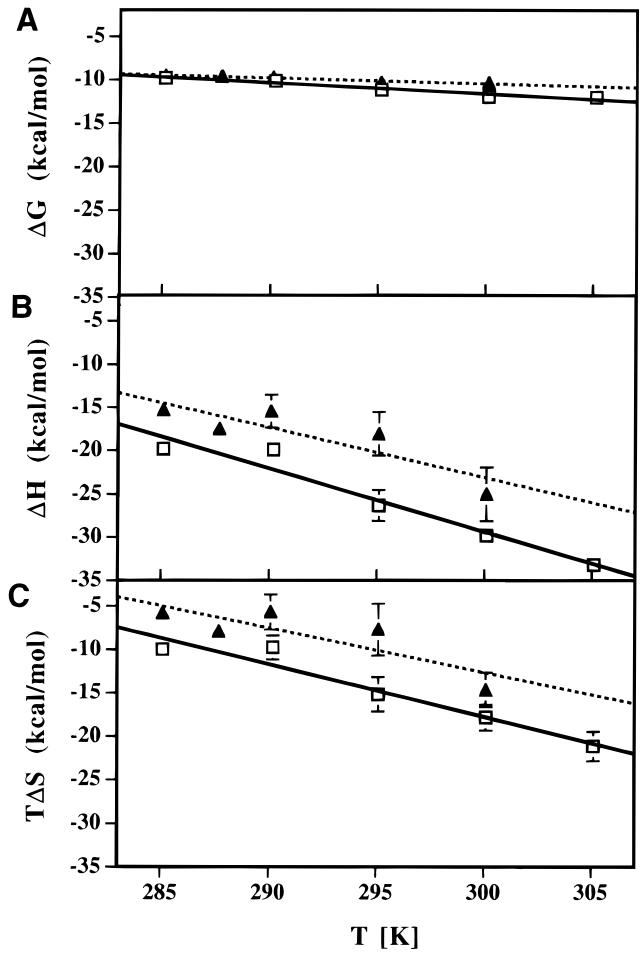

FIGURE 5: Thermodynamic profiles of the DNA binding reaction of MASH−BHLH in low-salt MES buffer as determined by titration calorimetry. (A) Plot of the free energy of binding, ΔG, against the temperature for titrations of MCK-S (□) and SP-1 oligonucleotide (▲) with MASH−BHLH. (B and C) Plots of the enthalpy ΔH (B) and of $T\Delta S$ (C) against the temperature for titrations of MCK-S (□) and SP-1 oligonucleotide (▲) with MASH−BHLH. ΔC_p was calculated by linear regression from the values for ΔH. The equation of linear regression fit was $\Delta H = -0.773\ (\pm 0.099)T + 190.4\ (\pm 29.5)$; $R^2 = 0.95$.

of the TATA binding protein (*21*) and of the transcription factor GCN4 (*19*).

The DNA binding reaction of MASH−BHLH showed a strong dependence on the reaction temperature of the measured enthalpy ΔH (Figure 5B) and of the derived $T\Delta S$ (Figure 5C), which compensate to make ΔG (Figure 5A) almost temperature-insensitive, at least within the range studied (Table 1). Such a behavior has been consistently observed for specific protein−DNA interactions (*22*−*27*). It is expected for any process which involves water as a solvent and which is characterized by a relatively large ΔC_p (vide infra) (*22*).

A notable feature of the binding reaction of MASH−BHLH is the fact that T_H, the temperature at which the reaction enthalpy equals zero, is −13 °C for binding to specific and nonspecific DNA in low-salt MES buffer (Figure 5B). T_H is also well below 0 °C in high-salt MES buffer (Table 1). The value of T_S, the temperature at which the reaction entropy changes sign, is −2 °C for E-box-containing DNA and +2 °C for heterologous DNA (Figure 5C).

Many other analyses of specific interactions between proteins and DNA indicated that the change of the driving force of the reaction took place within the physiological temperature range so that the binding reaction is entropically driven at low temperatures, but enthalpically driven at higher temperatures (*21*, *23*, *28*). Our results indicate a different behavior for the interactions of MASH−BHLH with DNA. Although the entropy changes are favorable at very low temperatures and strongly unfavorable at high temperatures (Figure 5C), the DNA binding reaction of MASH−BHLH is enthalpy driven throughout the physiologically relevant temperature range under the conditions used in this study (Figure 5B). A few examples of enthalpically driven association reactions have been described in the literature (*19*, *20*, *22*).

As mentioned above, the enthalpies of the binding reaction showed a strong dependence on the temperature. In good agreement with the data reported in Figure 5B, heat capacity changes were calculated under the assumption that ΔC_p was temperature independent in the small temperature range studied. Linear regression of the data in Figure 5B gave $\Delta C_p = -733\ (\pm 99)$ cal mol^{-1} K^{-1} for the MCK-S oligonucleotide and $\Delta C_p = -575\ (\pm 105)$ cal mol^{-1} K^{-1} for the SP-1 oligonucleotide. These values are comparable to the values reported for other association reactions between DNA and proteins (*23*, *24*, *27*, *29*, *30*). Large negative ΔC_p values have first been encountered in protein folding. They are now considered typical of specific protein−DNA recognition based on the stereospecific interaction of the complementary protein−DNA interface (*23*, *31*).

Coupling of MASH−BHLH Folding to DNA Binding. Changes in the exposure of nonpolar surface area are the major contributors to the heat capacity changes of DNA binding reactions (*32*, *33*). However, a more detailed analysis revealed that ΔC_p also contains contributions from the changes in the water accessibility of the polar surface area (*26*). Under the assumption that the change in polar surface area is approximately 59% of the change in nonpolar surface area—an assumption which is justified in many binding reactions (*26*, *27*, and references cited therein, *19*)—an empirical correlation between ΔC_p and the entropy change of the binding reaction due to the hydrophobic effect, ΔS_{HE}, could be derived (*26*). ΔS_{HE} for the reaction between MASH−BHLH and the MCK-S oligonucleotide was calculated to be 357 cal K^{-1} mol^{-1}. Due to the uncertainty in the ratio of the polar and the nonpolar water-accessible surface area, the error in ΔS_{HE} is likely to be approximately 10% (*27*). However, it must be kept in mind that the direct calculation of ΔS_{HE} is also rather inaccurate mainly due to the significant error introduced through the determination of the surface area from structural data.

The unfavorable entropic term ΔS_{RT} resulting from the reduction in the available rotational and translational degrees of freedom of MASH−BHLH and the oligonucleotide upon association was assumed to be independent of T_S and the molecular mass of the reactants. A value of −50 cal K^{-1} mol^{-1} was used (*27*, *34*). The conformation of the DNA is not changed significantly upon binding to BHLH proteins such as MASH-1, and it remains essentially in the B-form (Figure 6) (*6*, *7*, *9*, *10*, *12*, *14*, *35*, and data not shown). Under these assumptions, the entropy change resulting from local protein folding transitions coupled to DNA binding and the

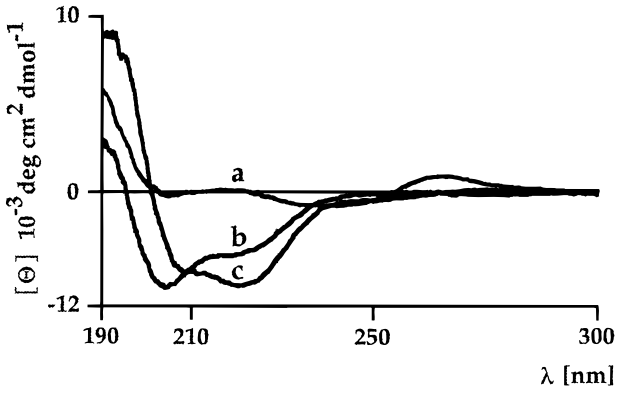

FIGURE 6: Characterization of the conformational behavior of MASH−BHLH by CD spectroscopy. Curve a, 50 μM MCK-S oligonucleotide (no protein present); curve b, 100 μM MASH−BHLH; curve c, mixture of 50 μM MCK-S and 100 μM MASH−BHLH (equivalent to 50 μM MASH−BHLH dimer). The contribution from the free oligonucleotide (curve a) was subtracted from the spectrum of the complex.

number of residues involved in the folding transition could be calculated as 307 cal mol^{-1} K^{-1} and 54, respectively (*27*). MASH−BHLH binds to DNA as a symmetrical dimer (vide supra) (*12*), and therefore 27 amino acid residues of each subunit undergo a transition from an unordered to a well-defined conformation upon DNA binding. Inspection of Figure 1A reveals that the N-terminal 27 amino acids comprise the entire basic domain, which is known to interact directly with DNA (*6*, *7*), and the N-terminal 2 amino acids of helix-1. Because we have neglected the contribution to the observed entropy change from the polyelectrolyte effect, ΔS_{PE} (*36*, *37*), the value reported might represent an upper limit for the actual number of residues undergoing a folding transition. Typical values for ΔS_{PE} are between 10 and 60 cal mol^{-1} K^{-1} (*27*). Measurements of the dependence of the equilibrium constant on the salt concentration by EMSA (data not shown) gave a value of 50 cal mol^{-1} K^{-1} for ΔS_{PE} in low-salt buffer (*38*), resulting in an increase of approximately 15% in the number of amino acid residues which change conformation upon complex formation. In summary, the ITC data suggest that DNA binding of the MASH−BHLH dimer is coupled to local folding of approximately 25 amino acid residues.

In agreement with these data, nuclear magnetic resonance studies of the BHLH protein E47 showed that the basic region was in a random coil conformation in the absence of DNA even at the millimolar concentrations used in the NMR experiments (*39*). The structure of the helix−loop−helix domain of the E47 homodimer, on the other hand, was preserved in solution when compared to the cocrystal structures of E47 and DNA (*7*).

CD Spectroscopic Studies of the Binding Reaction. The nature of the change in the conformation of MASH−BHLH upon DNA binding was further studied by circular dichroism spectroscopy. The CD spectrum of a 100 μM solution of MASH−BHLH showed that, in the absence of DNA, the protein adopted a conformation which was approximately 50% α-helical and 50% random coil (Figure 6) (*40*, *41*). Increasing the MASH−BHLH concentration did not change the CD spectrum. According to the X-ray analyses of the DNA complexes of MyoD and E47, the unstructured loop connecting helix 1 and helix 2 consists of approximately eight residues (*6*, *7*). Therefore, an additional 26 of the 68 amino acids of MASH−BHLH were in an unstructured conformation in the absence of DNA.

The CD spectrum of equimolar amounts of the MASH−BHLH dimer and double-stranded MCK-S oligonucleotide revealed a conformational change in part of the protein, in that the amount of α-helicity was increased to approximately 85%, or 58 of the 68 amino acid residues (Figure 6). Similar results were obtained for the addition of 1 equiv of SP-1 oligonucleotide to a solution of MASH−BHLH (data not shown). This observation could be explained with the formation of an α-helix in about 25 residues in the basic region of MASH−BHLH upon DNA binding. It agreed well with the results obtained from the ITC experiments.

Earlier results had shown that MASH−BHLH was largely unfolded at the concentrations where DNA binding occurs but adopted a mainly α-helical structure in the presence of DNA (*12*, *14*). Similarly, at least part of the BHLH domain was found to fold upon dimerization (*14*), and under the conditions of the ITC experiments, MASH−BHLH was found to be mainly dimeric with the dimerization mediated through the stably folded helix−loop−helix domain. However, the experiments described above indicate that the basic region is unfolded even under the high concentration conditions of the ITC experiments. In this context, it is worthy of note that unfavorable interactions are formed between the positive charges of the side chains of arginines 119, 120, 123, and 127 when the basic region of MASH−BHLH forms an α-helix in the absence of DNA. However, according to the X-ray structures of the DNA complexes of MyoD and E47 (*6*, *7*), the α-helicity of the basic region allows these arginine residues to form stabilizing interactions with the DNA phosphate backbone, thereby also reducing the repulsive interactions between them.

In summary, ITC experiments, which, unlike other DNA binding assays such as EMSA, filter binding experiments, or competitive DNA footprinting, are not inferential, have shown that MASH−BHLH binds to DNA with low sequence specificity. The binding reaction is enthalpically driven throughout the whole physiological temperature range. Dissection of the large negative heat capacity change measured for the binding reaction and CD spectroscopy indicated that the basic domain adopted an α-helical conformation only upon DNA binding. The X-ray structures of the DNA complexes of MyoD (*6*) and E47 (*7*) revealed that the BHLH proteins form a "clamp" which wraps around the DNA. Therefore, a large kinetic barrier would be expected for the association and dissociation reactions unless the helix in the basic region was not preformed in the free protein (*42*). A similar situation is found in the binding reaction of λ-repressor where the N-terminal arm, which wraps around the DNA in the operator complex, is flexible in solution (*43*), and in the transcriptional activators GCN4 and C/EBP (*19*, *44*, *45*).

The association reaction between MASH−BHLH and DNA could follow one of two mechanistic pathways. In the first, electrostatic guidance directs the strongly positively charged basic regions of the monomeric MASH−BHLH subunits to the DNA binding sites. This interaction facilitates the favorable interaction between the two HLH domains which is necessary for dimerization. Such a mechanism is followed, for example, by certain basic zipper proteins (*46*).

In the second possible association mechanism, the MASH−BHLH dimer is formed before it binds to DNA. We propose that this second mechanism is followed within the context of the cell. MASH-1 and the members of the MEF-2 family of transcription factors synergistically activate transcription, and this synergy is dependent on the direct physical interaction of the two DNA binding domains (*47*, *48*). Such an interaction might lock MASH−BHLH in the dimeric form and prevent dissociation into the monomeric subunits even at concentrations well below the dimerization constant.

ACKNOWLEDGMENT

We thank H. R. Bosshard for the use of his IT calorimeter and P. L. Luisi for the use of the CD spectrometer; C. Berger for introducing us to the experimental details of ITC; Lesley A. Tannahill and S. A. Benner for critical reading of the manuscript; and C. Berger and the members of our laboratory for helpful discussions.

REFERENCES

1. Sommer, L., Shah, N., Rao, M., and Anderson, D. J. (1995) *Neuron 15*, 1245−1258.
2. Molkentin, J. D., and Olson, E. N. (1996) *Curr. Opin. Gen Dev. 6*, 445−453.
3. Aplan, P. D., Nakahara, K., Orkin, S. H., and Kirsch, I. R. (1992) *EMBO J. 11*, 4073−4081.
4. Lassar, A. B., Davis, R. L., Wright, W. E., Kadesch, T., Murre, C., Voronona, A., Baltimore, D., and Weintraub, H. (1991) *Cell 66*, 305−315.
5. Johnson, J. E., Birren, S. J., and Anderson, D. J. (1990) *Nature 346*, 858−861.
6. Ma, P. C. M., Rould, M. A., Weintraub, H., and Pabo, C. O. (1994) *Cell 77*, 451−459.
7. Ellenberger, T., Fass, D., Arnaud, M., and Harrison, S. C. (1994) *Genes Dev. 8*, 970−980.
8. Lassar, A. B., Buskin, J. N., Lockshon, D., Davis, R. L., Apone, S., Hauschka, S. D., and Weintraub, H. (1989) *Cell 58*, 823−831.
9. Ferré-D′Amaré, A. R., Prendergast, G. C., Ziff, E. B., and Burley, S. K. (1993) *Nature 363*, 38−45.
10. Ferré-D′Amaré, A. R., Pognone, P., Roeder, R. G., and Burley, S. K. (1994) *EMBO J. 13*, 180−189.
11. Brownlie, P., Ceska, T. A., Lamers, M., Romier, C., Stier, G., Teo, H., & Suck, D. (1997) *Structure 5*, 509−520.
12. Meierhans, D., el Ariss, C., Neuenschwander, M., Sieber, M., Stackhouse, J. F., and Allemann, R. K. (1995) *Biochemistry 34*, 11026−11036.
13. Künne, A. G. E., Meierhans, D., and Allemann, R. K. (1996) *FEBS Lett. 391*, 79−83.
14. Künne, A. G. E., and Allemann, R. K. (1997) *Biochemistry 36*, 1085−1091.
15. Ladbury, J. E., and Chowdhry, B. Z. (1996) *Chem. Biol. 3*, 791−801.
16. Buskin, J. N., and Hauschka, S. D. (1989) *Mol. Cell. Biol 9*, 2627−2640.
17. Wetlaufer, D. R. (1962) *Adv. Protein Chem. 17*, 303−390.
18. Wiseman, T., Williston, S., Brandts, J. F., and Lin, L.-N. (1989) *Anal. Biochem. 179*, 131−137.
19. Berger, C., Jelesarov, I., and Bosshard, H. R. (1996) *Biochemistry 35*, 14984−14991.
20. Ladbury, J. E., Wright, J. G., Strutevant, J. M., and Sigler, P. B. (1994) *J. Mol. Biol. 238*, 669−681.
21. Petri, V., Hsieh, M., and Brenowitz, M. (1995) *Biochemistry 34*, 9977−9984.
22. Merabet, P. E., and Ackers (1995) *Biochemistry 34*, 8554−8563.
23. Ha, J.-H., Spolar, R. H., and Record, M. T., Jr. (1989) *J. Mol. Biol. 209*, 801−816.
24. Takeda, Y., Ross, P. D., and Mudd, C. P. (1992) *Proc. Natl. Acad. Sci. U.S.A. 89*, 8180−8184.
25. Murphy, K. P., and Freire, E. (1992) *Adv. Protein Chem. 43*, 313−361.
26. Spolar, R. S., Livingstone, J. R., and Record, M. T., Jr. (1992) *Biochemistry 31*, 3947−3955.
27. Spolar, R. S., and Record, M. T., Jr. (1994) *Science 263*, 777−784.
28. Foguel, D., & Silva, J. L. (1994) *Proc. Natl. Acad. Sci. U.S.A. 91*, 8244−8247.
29. Jin, L., Yang, J., and Carey, J. (1993) *Biochemistry 32*, 7302−7309.
30. Lundbäck, T., Cairns, C., Gustafsson, J.-A., Carlstedt-Duke, J., and Härd, T. (1993) *Biochemistry 32*, 5074−5082.
31. Burley, S. K. (1994) *Nat. Struct. Biol. 1*, 207−208.
32. Baldwin, R. L. (1986) *Proc. Natl. Acad. Sci. U.S.A. 83*, 8069−8072.
33. Sturtevant, J. M. (1977) *Proc. Natl. Acad. Sci. U.S.A. 74*, 2236−2240.
34. Finkelstein, A. V., and Janin, J. (1989) *Protein Eng. 3*, 1−3.
35. Allemann, R. K., and Egli, M. (1997) *Chem. Biol. 4*, 643−650.
36. Record, M. T., Jr., Lohman, T. M., and deHaseth, P. L. (1976) *J. Mol. Biol. 107*, 145−158.
37. Record, M. T., Jr., Ha, J.-H., and Fisher, M. (1991) *Methods Enzymol. 208*, 291−343.
38. Record, M. T., Jr., deHaseth, P. L., and Lohman, T. M. (1977) *Biochemistry 16*, 4791−4796.
39. Fairman, R., Beran-Steed, R. K., and Handel, T. M. (1997) *Protein Sci. 6*, 175−184.
40. Greenfield, N., and Fasman, G. D. (1969) *Biochemistry 8*, 4108−4116.
41. Compton, L. A., and Johnson, W. C., Jr. (1986) *Analytical Biochem. 155*, 155−167.
42. Sauer, R. T. (1990) *Nature 347*, 514−515.
43. Jordan, S., and Pabo, C. O. (1988) *Science* 895−899.
44. O'Neil, K. T., Shumann, J. D., Ampe, C., and DeGrado, W. F. (1991) *Biochemistry 30*, 9030−9034.
45. Weiss, M. A., Ellenberger, T., Wobbe, C. R., Lee, J. P., Harrison, S. C., and Struhl, K. (1990) *Nature 347*, 575−578.
46. Metallo, S. J., and Schepartz, A. (1997) *Nat. Struct. Biol. 4*, 115−117.
47. Black, B. L., Ligon, K. L., Zhang, Y., and Olson, E. N. (1996) *J. Biol. Chem. 271*, 26659−26663.
48. Mao, Z., and Nadal-Ginard, B. (1996) *J. Biol. Chem. 271*, 14371−14375.
49. German, M. S., Blanar, M. A., Nelson, C., Moss, L. G., and Rutter, W. J. (1991) *Mol. Endocrinol. 5*, 292−299.
50. Davis, R. L., Weintraub, H., and Lassar, A. B. (1987) *Cell 51*, 987−1000.

BI9725374